Genotoxicity Evaluation of Nanomaterials: DNA Damage, Micronuclei, and 8-Hydroxy-2-deoxyguanosine Induced by Magnetic Doped CdSe Quantum Dots in Male Mice

ARTICLE *in* CHEMICAL RESEARCH IN TOXICOLOGY · MARCH 2011

Impact Factor: 3.53 · DOI: 10.1021/tx2000015 · Source: PubMed

5 AUTHORS, INCLUDING:

Wagdy K B Khalil
National Research Center, Egypt
75 PUBLICATIONS **267** CITATIONS
SEE PROFILE

Emad Girgis
Harvard University
51 PUBLICATIONS **637** CITATIONS
SEE PROFILE

Mona B. Mohamed
Cairo University
76 PUBLICATIONS **3,679** CITATIONS
SEE PROFILE

K V Rao
KTH Royal Institute of Technology
468 PUBLICATIONS **6,348** CITATIONS
SEE PROFILE

Chemical Research in Toxicology

ARTICLE

pubs.acs.org/crt

Genotoxicity Evaluation of Nanomaterials: DNA Damage, Micronuclei, and 8-Hydroxy-2-deoxyguanosine Induced by Magnetic Doped CdSe Quantum Dots in Male Mice

W. K. B. Khalil,[*,†] E. Girgis,[‡,§] A. N. Emam,[§] M. B. Mohamed,[∥] and K. V. Rao[⊥]

[†]Cell Biology Department, National Research Center, 12622 Dokki, Giza, Egypt

[‡]Solid State Physics Department, National Research Center, 12622 Dokki, Giza, Egypt

[§]Advanced Materials and Nanotechnology Lab, CEAS, National Research Center, 12622 Dokki, Giza, Egypt

[∥]National Institute of Laser Enhanced Science, Cairo University, Egypt

[⊥]Department of Materials Science, Royal Institute of Technology, Stockholm S-100 44, Sweden

ABSTRACT: Quantum dots (QDs) are a novel class of inorganic fluorophores which are gaining widespread recognition as a result of their exceptional photophysical properties and their applications as a biomarker and in molecular biomedical imaging. The aim of this study was to evaluate the *in vivo* genotoxicity in mice exposed to CdSe quantum dots of average size 5.0 ± 0.2 nm and CdSe doped with 1% cobalt ions of similar size. The quantum dots are surface modified using mercaptoacetic acid (MAA) in order to be biocompatible and water-soluble. The MAA-QDs were given to the mice orally at doses of 500, 1000, and 2000 mg/kg by weight of MAA-QDs. Bone marrow and liver samples were collected after two and seven days of treatment. The results indicated that after two days of treatment, the high dose of doped MAA-QDs was significantly able to induce DNA damage, formation of micronuclei (MNs), and generation of DNA adduct (8-hydroxy-2-deoxyguanosine, 8-OHdG). However, increasing DNA damage and the frequency of MNs formation as well as the generation of DNA adducts were observed with both the undoped MAA-QDs (2000 mg/kg) and doped MAA-QDs (1000 and 2000 mg/kg) after seven days of treatment. The results of our study indicate that exposure to high doses of pure MAA-QDs or MAA-QDs doped with cobalt has the potential to cause indirect *in vivo* genetic damage, which may be attributed to free radical-induced oxidative stress in mice.

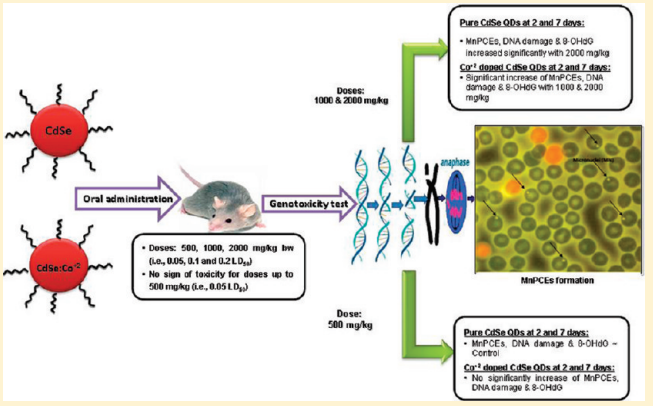

1. INTRODUCTION

Semiconductor nanocrystals, also named quantum dots (QDs), have attracted a lot of attention in the past few decades due to their unique optical properties, which make them ideal optical probes for use in biomedicine and biotechnology.[1−5]

Quantum dots are inorganic semiconductors that are confined in three dimensions, typically spheres with a diameter in the range of 2−10 nm.[6] They have unique optical and electronic properties such as bright fluorescence, broad excitation spectrum, narrow/symmetric emission spectrum, and high photostability.[7−9] In 1998, two pioneering research articles came out by Bruchez et al.[1] and Chan and Nie[10] demonstrating the possible applications of QDs as biomarkers in *in vivo* biomedical imaging. Since that time, the use of QDs has been demonstrated in biology and medicine as fluorescent probes and more recently in analytical chemistry.[11−18]

The current widely used organic fluorophores, used as biological labels for fluorescence imaging and detection, have shortcomings associated with their fluorescence. Signals from the labeled molecules can be obscured by cell auto fluorescence, occurring in the visible spectrum, and by photobleaching, which seriously limits the observation time. Semiconductor QDs have unique optical and electronic properties which makes them superior for biomedical imaging such as tunable band gap, brighter images, and photostable fluorophores of a few nanometers in diameter. By controlling their sizes, fluorescence emission could be tuned from the visible to infrared (IR) region. Furthermore, QD surface modification gives these nanoparticles strong binding affinity toward protein and DNA molecules and consequently great advantages for *in vivo* biomedical imaging and early diagnosis of disease.[1,10] QDs have some harmful constituents such as cadmium or selenium that are toxic to many cells. The potential toxic effects of these QDs have recently become a topic of considerable importance and discussion. Dubertret et al.[19] reported the effects of CdSe/ZnS core−shell QDs on the development of individual cells of early stage *Xenopus*

Received: September 20, 2010
Published: March 22, 2011

embryos. They found CdSe/ZnS core−shell QDs at low concentrations have little effect on cell viability, morphology, function, and development over the duration of the experiments. However, at higher concentrations, CdSe/ZnS core−shell QDs have noticeable effects on embryo development. They thought that these abnormalities may result from changes in the osmotic equilibrium of the cells due to the injected CdSe/ZnS core−shell QDs. Derfus et al.[20] probed the cytotoxicity of CdSe QDs using primary hepatocytes as a liver model. They found that the cytotoxicity of CdSe QDs correlated with the liberation of free Cd^{2+} ions due to deterioration of the CdSe lattice. Yamamoto and co-workers developed several novel surface-modified QDs using carboxylic acids, polyalcohols, and amines and evaluated their cytotoxicity in mammalian cells.[21] They believed that the cytotoxicity of QDs is caused by the capping molecules of QDs but not by the CdSe nanocrystals themselves. Parak and co-workers investigated the effect of different organic shells on cytotoxicity.[22] They found that the aggregation of CdSe QDs plays an important role in cytotoxic effects, as well as the release of toxic Cd^{2+} ions from the particles. Lovrić et al.[23] examined the subcellular localization and toxicity of CdTe QDs. The results showed that QD-induced cytotoxicity is in partly dependent on QD size and is characterized by chromatin condensation and membrane blebbing. In addition, cytotoxicity of QDs could be significantly reduced by the treatment of cells with *N*-acetylcysteine or bovine serum albumin. Green and Howman reported DNA damage in plasmid nicking assays with water-soluble CdSe/ZnS core−shell QDs.[24] They also suggested a mechanism based on the observed free radical generation.

A problem associated with the use of QDs as a biomarker is their capacity for blinking. This phenomenon is attributed to material defects or dangling bonds on the surface of the QDs.[25−29] This is a natural consequence of the large surface-to-volume ratio of the sub-10-nanometer particles. These material defects lead to disorders in the electronic states that lie within the material's energy gap. Electrons can relax into these states, whereupon they typically undergo either nonradiative or radiative decay to the ground state. Thus, the surface defects introduce carrier losses that inhibit the optical fluorescence. To avoid this problem, investigators previously used coating consisting of higher band gap materials to increase the luminescence efficiencies of QDs. Coating CdSe nanocrystals by another shell of ZnS enhances their emission properties.[30−33] In order to use these particles for *in vivo* biomedical application, they must be water-soluble and biocompatible; therefore, surface modifications are required. Despite the previous citation, there are very few studies performed on the influence of CdSe QDs on DNA damage in mammals *in vivo*. Doping with Co^{2+} ions is expected to eliminate blinking phenomena.[34] Therefore, the main objective of the present study was to investigate the *in vivo* genotoxicity of pure MAA-QDs and Co^{2+}-doped MAA-QDs in the liver and the bone marrow cells of male mice.

2. EXPERIMENTAL PROCEDURES

2.1. Materials. The materials used were cadmium oxide {(CdO), Fluka, 99%}, Se powder {(Se), Riedel, 99%}, cobaltous chloride hexahydrate ($CoCl_2.6H_2O$, WINLAB, 98%), trioctyl phosphine {(TOP), Fluka, 90%}, stearic acid {($CH_3(CH_2)_{16}COOH$), Fluka 98%}, hexadecyl amine {(HDA), Aldrich 97%}, trioctyl phosphine oxide {(TOPO), Fluka 97% and Merck 97%}, hydrazine hydrate {($N_2H_4.H_2O$), Fine Chemicals LTD 80%}, carbon disulfide {(CS_2), Fluka 99.8%}, methanol {(CH_3OH), Sigma 99%}, and mercapto-acetic acid {(MAA), Fine Chemicals LTD 80%}.

CdSe QDs were prepared by the method reported earlier;[35−37] a mixture of CdO and stearic acid was heated up until the CdO completely dissolved and the red color disappeared. The Se-TOP solution was injected quickly into the reaction flask at 250 °C. The color of the solution changes to orange due to the formation of CdSe quantum dots. The formed particles were separated from the reaction mixture by adding methanol and then centrifuged. The particles were precipitated out and removed from the reaction mixture, then redispersed in toluene.

CdSe QDs doped with Co^{2+} were prepared as described above, but 1% cobalt dithiocarbazate complex was mixed with the mixture of CdO and stearic acid.

The doped and undoped CdSe QDs are water insoluble because they are capped with TOPO. These particles were surface modified using mercapto-acetic acid (MAA) to be water-soluble and biocompatible and also to remove the TOPO molecules. The modification was carried out as follows: in a typical method, 0.1 g of prepared CdSe QDs powder (doped or undoped) was dissolved in 5 mL of toluene, then 1 mL of methanol solution which contains 0.2 g MAA was added. This mixture was refluxed at 60 °C with constant stirring for 3 h until TOPO was totally replaced by MAA molecules as shown in Figure 1. The MAA coated doped and undoped CdSe QDs were separated by centrifugation and washed several times with a water−methanol mixture to ensure the removal of all TOPO molecules. These particles were redispersed into phosphate buffered saline (PBS).

The particle size and shape were characterized using high resolution transmission electron microscopy (HR-TEM) JEM 2100 LB_6 under an operating voltage of 200 kV to investigate the micrograph of prepared doped and undoped QDs under an operating voltage of 200 kV for different samples. The optical properties such as UV−visible absorbance spectra of prepared doped and undoped QDs have been investigated using a Perkin-Elmer Lambda 40 double beam spectrophotometer. The absorption was recorded within the appropriate scan range from 200 to 900 nm, and the photoluminescence spectra of the diluted solution of prepared doped and undoped QDs (with an optical density below 0.1) were recorded using UV-quartz cuvettes of 1×1 cm^2 using a Perkin-Elmer LS55 spectrofluorimeter. The excitation wavelength was 410 nm, the slit width was 10 nm, and the scan speed was 500 nm. The photoluminescence was recorded within the appropriate scan range from 500 to 900 nm. Finally, the magnetic measurements were carried out using a vibrating sample magnetometer (VSM; ADE Technologies, Inc. EV11; model 8810). Particle size and distribution of the original solution and the concentrated solution were measured by dynamic light scattering (DLS), using Malvern Zetasizer Nano-ZS (Malvern Instruments Ltd., Worcestershire, UK).

2.2. Experimental Animals. One hundred and sixty adult male albino mice (20−25 g, purchased from the Animal House Colony, Giza, Egypt) were maintained on standard laboratory diet (protein, 16.04%; fat, 3.63%; fiber, 4.1%; and metabolic energy, 0.012 MJ) and water *ad libitum* at the Animal House Laboratory, National Research Center, Dokki, Giza, Egypt. After an acclimation period of 1 week, animals were divided into groups (10 mice/group) and housed individually in filter-top polycarbonate cages, housed in a temperature-controlled (23 ± 1 °C) and artificially illuminated (12 h dark/light cycle) room free from any source of chemical contamination. All animals received humane care in compliance with the guidelines of the Animal Care and Use Committee of National Research Center, Egypt.

2.3. Dose Preparations. The genotoxic effects of doped and undoped MAA-QDs were investigated in bone marrow and liver cells of male albino mice, using MN, DNA fragmentation, and DNA-adduct assays. An acute oral toxicity study based on Organisation for Economic Co-operation and Development (OECD) Guideline 420, updated and adopted on 15 November 2009,[38] of doped and undoped QDs was the basis for determination of doses. A single mouse was dosed first with a 5 mg/kg body weight (bw) single dose. If no mortality and no toxic

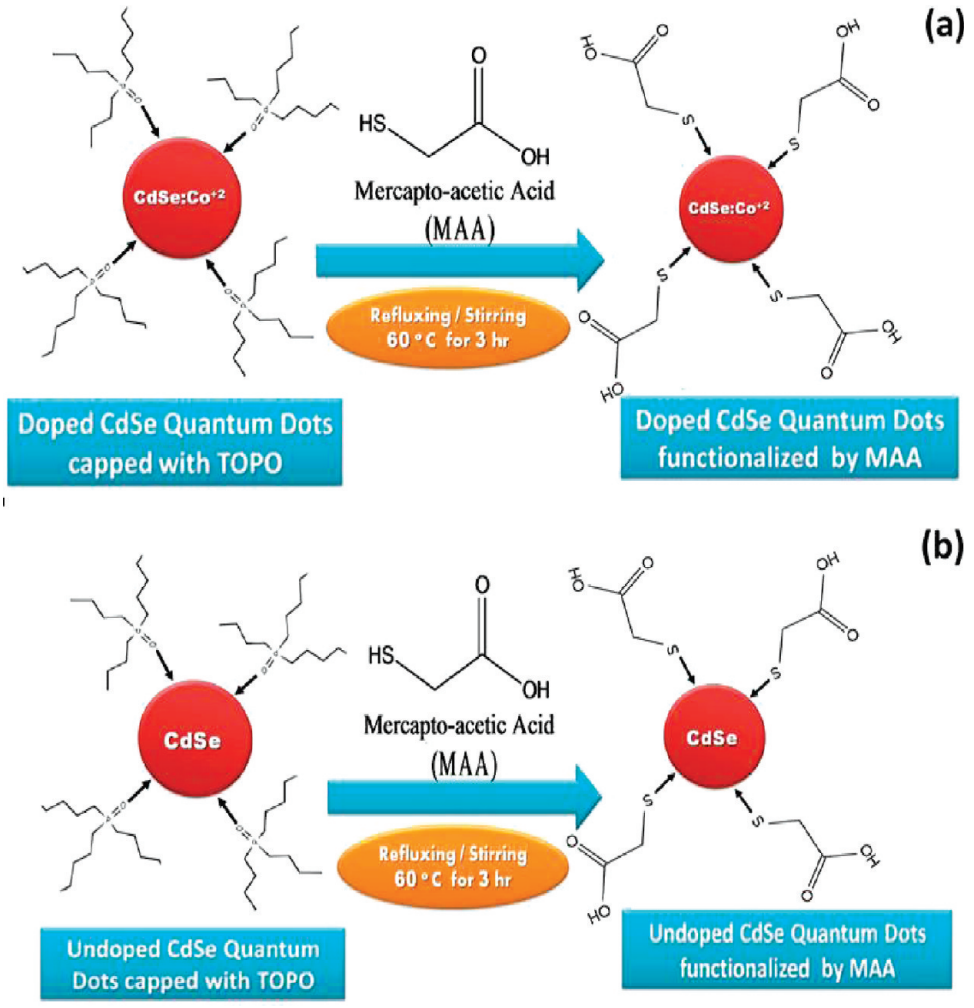

Figure 1. Schematic diagram shows the mechanism of surface functionalization replacement by using Co-doped CdSe QDs with a doping ratio 1% (a) and undoped CdSe MAA-QDs (b).

symptoms (loss of appetite and weakness) were found, the second mouse received a 50 mg/kg bw single dose, then 300 mg/kg bw and 2000 mg/kg bw single doses in sequence in the sighting study. Since no mortality and no toxic symptoms, which were determined through 2 weeks after injection, were found at any dose level in the pilot study, the dose was increased up to 50% lethal dose (LD_{50}, lethal dose that kills 50% of the animals). The LD_{50} of the MAA-QD or MAA-QD-Co was 10000 mg/kg bw. The main study with ten mice was done at 0.05, 0.1, and 0.2 LD_{50} of doped and undoped MAA-QDs, in which no mortality and no toxic symptoms were observed. Therefore, three dose levels of doped and undoped MAA-QDs, 500, 1000, and 2000 mg/kg bw (i.e., 0.05, 0.1, and 0.2 LD_{50}, respectively), were used for the mice liver DNA fragmentation, DNA-adduct formation, and bone marrow MN assays.

2.4. Experimental Design. The experimental design for the *in vivo* tests included four main groups: the control, the positive control (cyclophosphamide) group, and the experimental groups, including doped and undoped MAA-QDs. The experimental groups were divided into 3 subgroups each for the different doses 500, 1000, and 2000 mg/kg, respectively. All groups had the same number of animals per test. Thus, for DNA fragmentation, DNA-adduct formation, and MN assays, ten animals were used per dose and time intervals (2 and 7 days).

Institutional Animal Ethics Committee approved the study. Experimental doses of all groups were obtained by suspending 500, 1000, and 2000 mg/kg bw of doped and undoped MAA-QDs in a ultrapure bidistilled water (DDW)−Tween 80 mixture and administering it to the mice by oral gavage. All animals received a single oral dose. The control group was treated with a DDW−Tween 80 mixture. A known mutagen, cyclophosphamide at a dose of 40 mg/kg, bw, was used for the positive control group. It was given intraperitoneally (i.p.), and the volume injected was 0.01 mL/g bw. The animals were sacrificed after 2 and 7 days of the acute oral treatment with doped and undoped MAA-QDs. Bone marrow samples were collected from both femurs of each animal and extracted immediately and processed for the MN assay. The liver samples were immediately frozen at −20 °C prior to use for DNA fragmentation and DNA-adduct formation assays.

2.5. DNA Fragmentation Analysis. *2.5.1. Diphenylamine Reaction Procedure.* Mice liver tissues were used to determine the quantitative profile of the DNA fragmentation. Liver samples were collected immediately after sacrificing the animals. The tissues were lysed in 0.5 mL of lysis buffer containing, 10 mM tris-HCl (pH 8), 1 mM EDTA, and 0.2% triton X-100, centrifuged at 10 000 rpm (Eppendorf) for 20 min at 4 °C. The pellets were resuspended in 0.5 mL of lysis buffer. To the pellets (P) and the supernatants (S), 0.5 mL of 25% trichloroacetic acid (TCA) was added and incubated at 4 °C for 24 h. The samples were then centrifuged for 20 min at 10 000 rpm (Eppendorf) at 4 °C, and the pellets were suspended in 80 mL of 5% TCA, followed by incubation at 83 °C for 20 min. Subsequently, to each sample 160 mL of DPA solution [150 mg of DPA in 10 mL of glacial acetic acid, 150 mL of sulfuric acid, and 50 mL of

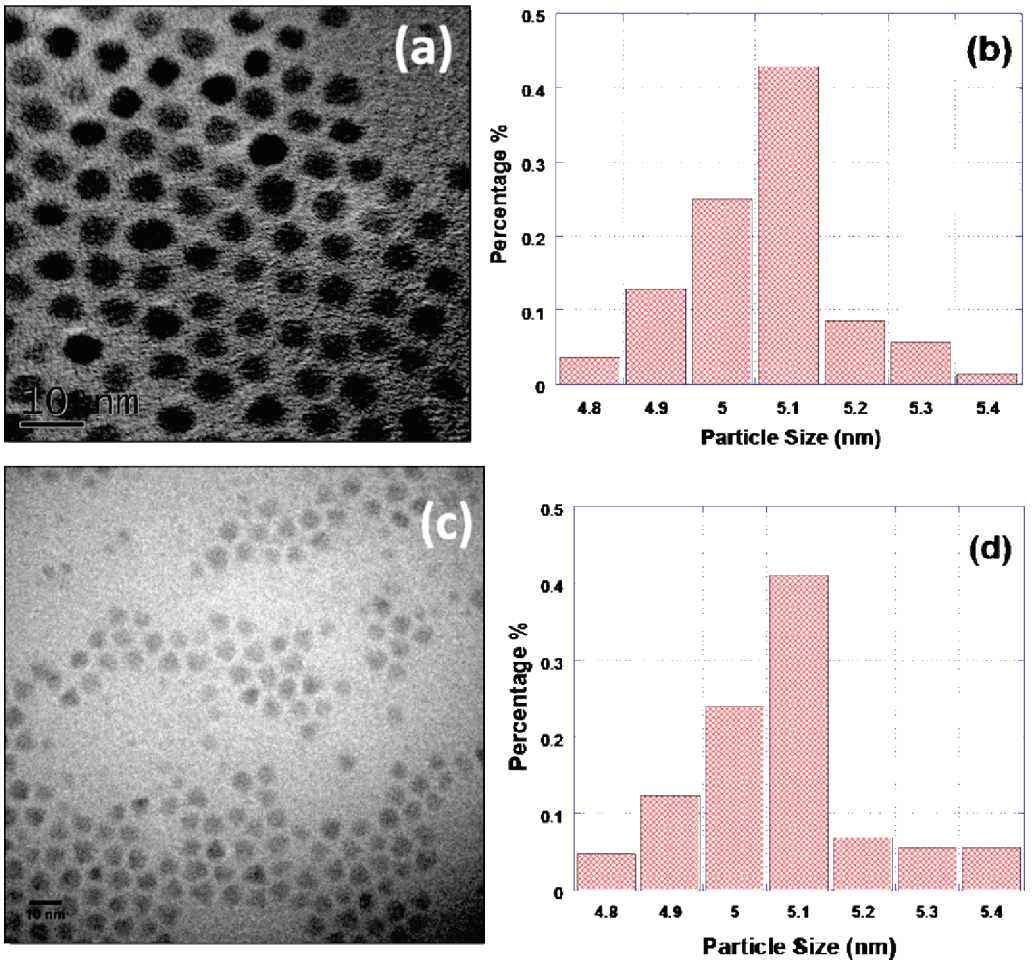

Figure 2. TEM images with different magnification and histograms for Co-doped CdSe QDs with a doping ratio of 1% (a,b) and undoped CdSe QDs (c,d).

acetaldehyde (16 mg:ml)] was added and incubated at room temperature for 24 h.[39] The proportion of fragmented DNA was calculated from an absorbance reading at 600 nm wavelength using the following formula:

$$\%\text{fragmented DNA} = \frac{\text{OD(S)}}{\text{OD(S)} + \text{OD(P)}} \times 100$$

2.5.2. DNA Gel Electrophoresis Laddering Assay. Apoptotic DNA fragmentation was qualitatively analyzed by detecting the laddering pattern of nuclear DNA as described according to Lu et al.[40] Briefly, liver tissues were homogenized, washed in PBS, and lysed in 0.5 mL of DNA extraction buffer (50 mM Tris−HCl, 10 mM EDTA. 0.5% Triton, and 100 μg/mL proteinase K, pH 8.0) overnight at 37 °C. The lysate was then incubated with 100 μg/mL DNase-free RNase for 2 h at 37 °C, followed by three extractions of an equal volume of phenol/chloroform (1:1 v/v), and a subsequent re-extraction with chloroform by centrifuging at 15,000 rpm for 5 min at 4 °C. The extracted DNA was precipitated in two volumes of ice-cold 100% ethanol with a 1/10 volume of 3 M sodium acetate, pH 5.2 at −20 °C for 1 h, followed by centrifuging at 15,000 rpm for 15 min at 4 °C. After washing with 70% ethanol, the DNA pellet was air-dried and dissolved in 10 mM Tris−HCl/1 mM EDTA, pH 8.0. The DNA was then electrophoresed on 1.5% agarose gel and stained with ethidium bromide in Tris/acetate/EDTA (TAE) buffer (pH 8.5, 2 mM EDTA, and 40 mM Tris−acetate). A 100-bp DNA ladder (Invitrogen, USA) was included as a molecular size marker, and DNA fragments were visualized and photographed by exposing the gels to ultraviolet transillumination.

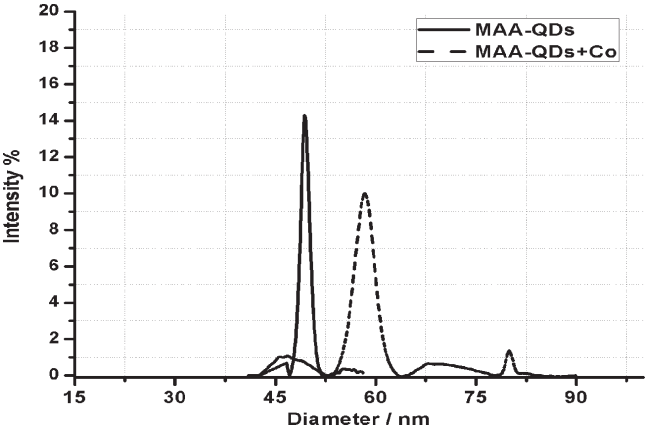

Figure 3. Size distribution by intensity, measured with DLS, of MAA-QDs in saline for Co-doped CdSe QDs with a doping ratio of 1% and undoped CdSe QDs.

2.6. Micronucleus Test by Acridine Orange Fluorescent Staining. Acridine orange staining of erythrocytes was performed according to Ueda et al.[41] To assess this assay, ten animals from each treatment were sacrificed after the exposure period. The bone marrow cells were collected from both femora and resuspended in a small volume of fetal calf serum (FBS; Sigma) on a 0.003% acridine orange-coated glass

dx.doi.org/10.1021/tx2000015 |*Chem. Res. Toxicol.* 2011, 24, 640–650

Table 1. DLS Data of the MAA-QDs and MAA-QDs+Co^{+2}

vehicles	diameter (nm) HD[a]	poly dispersity index	zeta potential (mV)	Ph
MAA-QDs in saline	48 nm	0.0689	−25.7	5.8
doped MAA-QDs+Co^{2+} in saline	58 nm	0.0408	−37.4	5.8

[a] HD is hydrodynamic diameter.

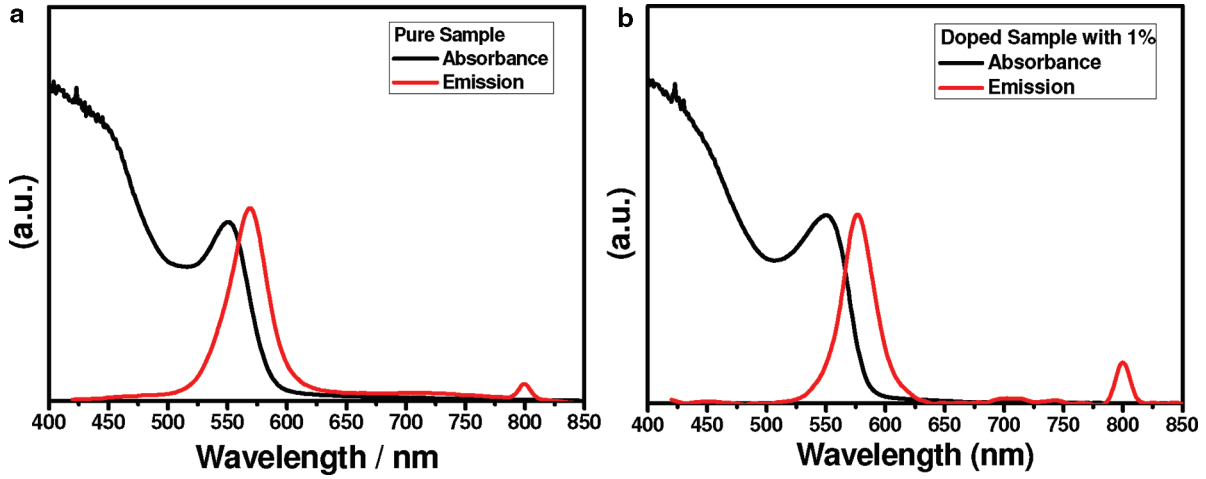

Figure 4. Optical properties for each of the undoped (pure) CdSe QDs and CdSe QDs doped with 1% of Co ions.

slide. The slide was then covered with a cover glass to prepare bone marrow specimens. Slides were dried overnight and fixed with methanol for 10 min. Bone marrow specimens were examined in a blind manner using fluorescence microscopy at 600× or higher magnification with a blue excitation wavelength (e.g., 488 nm) and yellow to orange barrier filter (e.g., 515 nm long pass). Two slides per animal were labeled to get blind micronuclei scoring. To avoid obtaining unbiased results, the slides were observed once by one observer who has sufficient experience of micronucleus tests. The number of micronucleated polychromatic erythrocytes (%MnPCEs) was measured at a rate of 3000 polychromatic erythrocytes (PCEs) per animal.

2.7. HPLC Measurement of 8-Hydroxy-2-deoxyguanosine (8-OHdG) and 2-Deoxyguanosine (2-dG). DNA was extracted from mice liver by homogenization in buffer containing 1% sodium dodecyl sulfate, 10 mM Tris, 1 mM EDTA (pH 7.4), and an overnight incubation in 0.5 mg/mL proteinase K at 55 °C. Homogenates were incubated with RNase (0.1 mg/mL) at 50 °C for 10 min and extracted with chloroform/isoamyl alcohol. The extracts were mixed with 3 M sodium acetate and two volumes of 100% ethanol to precipitate DNA at −20 °C. The samples were washed twice with 70% ethanol, air-dried for 15 min, and dissolved in 100 μL of 10 mM Tris/1 mM EDTA (pH 7.4). DNA digestion was performed as previously described.[42] The adduct 8-OHdG was measured with high-performance liquid chromatography (HPLC) equipped with a CoulArray system (Model 5600). Analytes were detected on two coulometric array modules, each containing four electrochemical sensors attached in series, which allows identification targets based on reduction potential. UV detection was set to 260 nm. HPLC was controlled and the data acquired and analyzed using CoulArray software. The mobile phase was composed of 50 mM sodium acetate/5% methanol at pH 5.2. Electrochemical detector potentials for 8- OHdG and 2-dG were 120/230/280/420/600/750/840/900 mV, and the flow rate was 1 mL/min.

2.8. Statistical Analysis. All data were analyzed using the general liner models (GLM) procedure of Statistical Analysis System[43] followed by the Scheffé test to assess significant differences between groups. The values are expressed as the mean ± SEM. All statements of significance were based on a probability of $P < 0.05$.

3. RESULTS

3.1. Quantum Dot Preparation, Characterization, and Surface Modification. The quality of the prepared quantum dots was ensured by measuring their optical properties and determining their particle size and shape using transmission electron microscopy (TEM). Magnetic measurement of the prepared particles using a vibrating sample magnetometer was carried out to ensure doping of the CdSe particle by Cobalt ions.

Figure 2 shows the TEM images of the prepared quantum dots associated with their histogram to show the sample quality and their size distribution. TEM images clearly show that the nanocrystals are dot-like in shape, highly uniform in size and shape for each of the doped and undoped QDs. In addition, the high contrast of the dot-like particles as shown in Figure 2a is due to the presence of magnetic dopant impurities from Co^{2+} ions in CdSe QDs, but the low contrast of the dot as in Figure 2c is due to undoped CdSe QDs. The average particle size is about 5.1 ± 0.2 nm as shown in the histogram of both TEM images Figure 2b and d).

Figure 3 shows DLS and electrophoretic mobility. We measured the size and zeta potential in a vehicle, as listed in Table 1. The pure MAA-QDs have a hydrodynamic diameter R of approximately 48 nm and 58 nm for MAA-QDs+Co^{2+}. The polydispersity indices for MAA-QDs and MAA-QDs+Co^{2+} are 0.0689 and 0.0408, respectively, depending on the vehicle. Moreover, the particles tended to aggregate, and this was more pronounced with MAA-QDs+Co^{2+} than with MAA-QDs, as illustrated in Figure 3. Both MAA-QDs and MAA-QDs+Co^{2+} have a negative zeta potential in all tested vehicles, but the MAA-QDs+Co^{2+} are 1.5-fold more negative than the MAA-QDs (Table 1). This is due to the formation of secondary size from cobalt nanoclusters in MAA-QDs+Co^{2+}.

Figure 4 shows the typical optical properties (absorption and emission spectra) for the prepared undoped and Co-doped CdSe

dx.doi.org/10.1021/tx2000015 |Chem. Res. Toxicol. 2011, 24, 640–650

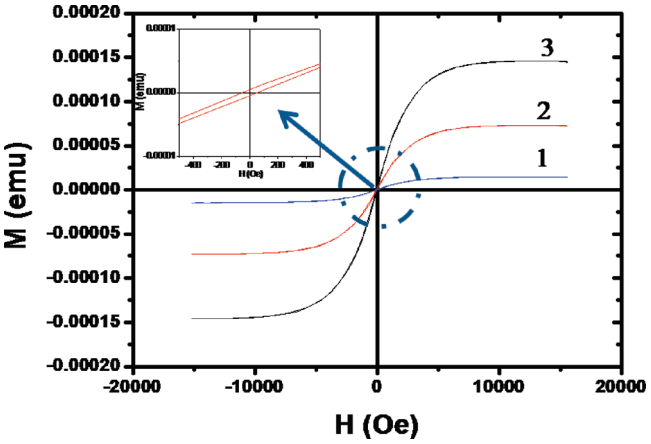

Figure 5. Magnetic behavior of Co-doped CdSe nanocrystals with a doping ratio 1% measured at different doses (1, 2, and 3 with doses 500, 1000, and 2000 mg/kg, respectively) at room temperature.

QDs with the same size. Figure 4a and b shows the first excitonic transition of the absorption spectra (maximum wavelength λ_{max} = 550 nm) of the undoped CdSe NCs (black line) with particle size = 5.5 nm calculated by Brus's equation.[44]

Figure 5 shows the magnetic hysteresis loops which confirm the existence of the magnetic impurity dopants inside the CdSe host crystals measured at room temperature (300 K). The samples were measured using a vibrating sample magnetometer (VSM) for Co-doped CdSe QDs with a doping ratio of 1%. Figure 5 shows three hysteresis loops for three different samples with different doses: 1, 2, and 3 (500, 1000, and 2000 mg/kg bw).

3.2. Genotoxcity of the QDs. *3.2.1. DNA Fragmentation.* Quantitative DNA fragmentation was determined in male mice exposed to several doses of doped and undoped MAA-QDs particles. The DNA damage was examined in liver tissues collected from MAA-QDs-treated mice using a gel electrophoresis laddering assay and a diphenylamine reaction procedure (Figures 6 and 7, respectively). The results of the gel electrophoresis laddering assay revealed that two days of MAA-QDs treatment caused similar DNA damage in all groups of undoped and doped QDs except the MAA-QD+Co2000 group (Figure 6). The MAA-QD+Co2000 group had more bands compared with the control and the other treated groups but less than cyclophosphamide-treated group (Figure 6a). However, the DNA damage increased seven days after treatment in undoped (MAA-QD2000) and doped (MAA-QD+Co1000 and MAA-QD+Co2000) groups compared to that in the control group. However, the DNA damage in these groups was lower than those in cyclophosphamide-treated group (Figure 6b).

The results of the diphenylamine reaction revealed that two days after undoped MAA-QDs treatment DNA damage was slightly higher than that in the control group. Undoped MAA-QDs produced a rate of DNA damage about 11 ± 1.0, 11.3. ± 0.7, and 12.9 ± 0.9% at 500, 1000, and 2000 mg/kg bw, respectively, compared to 9.1 ± 1% in control group (Figure 7a). However, DNA damage increased significantly at seven days after injection of the highest dose of undoped MAA-QDs compared with that in the control group (Figure 7b).

However, doped MAA-QDs were able to produce higher DNA fragmentation (14.9 ± 0.8 and 18.5 ± 0.9%) in the liver tissues treated by acute doses (1000 and 2000 mg/kg bw) of doped MAA-QDs two days after treatment than in the control group (9.1 ± 1%, Figure 7a). This increase in DNA damage was significantly different ($P < 0.05$, Figure 7a) only in the doped MAA-QD2000 group compared to the control group. Moreover, liver tissues collected from groups exposed to acute doses of doped MAA-QDs seven days after treatment showed a rate of DNA damage about 19.8 ± 0.9 and 24.9 ± 1.1% compared to that in the control group (9.2 ± 0.9%). This increase in DNA damage was significantly different ($P < 0.05$, Figure 7b). However, cyclophosphamide treated liver tissues showed a significantly increased rate of DNA damage in comparison to that in all other groups and for both time intervals (Figure 7a and b).

3.2.2. Micronucleus Assay. The effect of MAA-QDs on MnPCE formation in the bone marrow cells of male mice is summarized in Table 2 and Figure 8. The results revealed that after two and seven days of MAA-QDs treatment with 500 and 1000 mg/kg bw of undoped MAA-QDs MnPCE formation was similar to that in the control group. Treatment of male mice with 2000 mg/kg bw of undoped MAA-QDs increased the formation of MnPCEs at the two time intervals compared with that in the control group (Table 2). However, this increase of MnPCEs formation was significantly different with 2000 mg/kg bw of undoped MAA-QDs at seven days after treatment.

Exposure of male mice with low and medium doses of doped MAA-QDs at two days after treatment did not significantly increase the incidence of MnPCEs compared with that in the control group. However, treatment of male mice with the highest dose of doped MAA-QDs significantly increased the incidence of MnPCEs compared with that in the control group. In contrast, on the seventh day after treatment the formation of MnPCEs in the bone marrow cells of male mice treated by 1000 and 2000 mg/kg bw increased significantly compared with that of the control group (Table 2 and Figure 8).

3.2.3. MAA-QDs Induce 8-Hydroxy-2-deoxyguanosine (8-OHdG) Generation. Assessment of 8-OHdG generation in a hepatic mice genome following MAA-QDs treatment as a surrogate for oxidative stress induced damage is summarized in Figure 9. The results indicated that 8-OHdG levels in control liver tissues ranged from 3.4 8-OHdG per 10^5 dG to 3.5 8-OHdG per 10^5 dG (Figure 9a and b).

The 8-OHdG/2-dG ratio following a low dose of undoped MAA-QDs treatment at two and seven days was relatively similar to that of the control group. However, the ratio of 8-OHdG/2-dG generation increased to 1.6-fold following a medium dose of undoped MAA-QDs at seven days after treatment in comparison to that of the control group. In addition, this ratio increased from 1.7-fold at two days to 2.5-fold at seven days after undoped MAA-QDs treatment (Figure 9a and b).

In the same trend, the ratio of 8-OHdG/2-dG generation increased slightly following a low dose of doped MAA-QDs treatment at two and seven days compared with that in the control group (Figure 9a and b). However, the ratio of 8-OHdG/2-dG generation increased to 1.5- and 2.1-fold at two days to 2.6- and 3.7-fold at seven days following medium and high doses of doped MAA-QDs treatment, respectively (Figure 9a and b).

4. DISCUSSION

The aim of this study was to investigate the genotoxicity of pure and doped MAA-QDs. The factors taken into consideration for this study were (i) physicochemical properties of the particles, (ii) capability of the particles to induce genotoxicity in mice liver and bone marrow cells, and (iii) genomic damage caused by oxidative stress (8-OHdG).

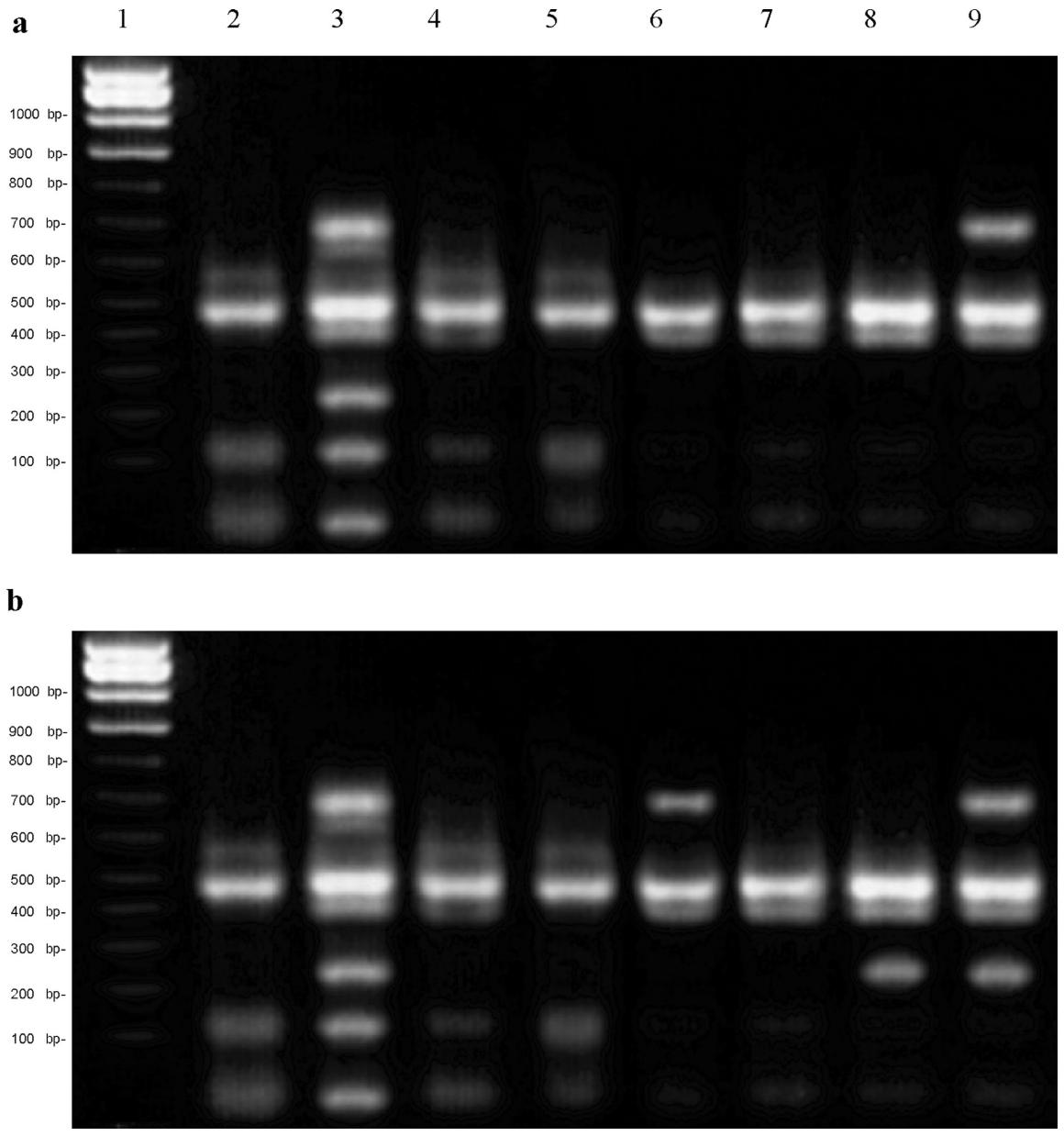

Figure 6. DNA fragmentation detected with agarose gel of DNA extracted from liver tissues of male mice collected after 2 (a) and 7 days (b) following oral treatment of MAA-QDs analyzed by a DNA gel electrophoresis laddering assay. Lane 1 represents the DNA ladder. Lane 2 represents control samples. Lane 3 shows DNA fragmentation in liver tissues following cyclophosphamide treatment. Lanes 4−6 show DNA fragmentation in liver tissues following oral treatment with 500, 1000, and 2000 mg/kg of undoped MAA-QDs, respectively. Lanes 7−9 show DNA fragmentation in liver tissues following oral treatment with 500, 1000, and 2000 mg/kg of doped MAA-QDs, respectively.

It is important to mention that the cobalt dithiocarbazate complex decomposes forming cobalt ions during the same temperature range at which Cd stearate organometallic salt decomposes. This leads to doping of CdSe nanocrystals with different ratios of cobalt. Moreover, the presence of localized magnetic ions in the semiconductor alloy leads to strong exchange interactions between (sp) band electrons and the magnetic ion (d) electrons. This (sp−d) exchange interaction constitutes a unique interplay between semiconductor and magnetism that plays a double role in determining the optical properties of these materials. This could enhance the emission properties of the quantum dots used as a biological label because this could eliminate the photodarkening effect (blinking phenomena) of the quantum dots.

Figure 4 shows the optical properties (absorption and emission spectra) of the prepared undoped and Co-doped CdSe QDs with the same particle size (5.5 nm). The emission spectrum (red line) where λ_{max} = 568 nm shows a perfect sample without any surface trap emission, and the stock shift is about 18 nm (Figure 4a). Figure 4b shows the absorption spectra of the CdSe QDs doped with 1% of Co^{2+} (black line) where λ_{max} = 550 nm. The emission spectrum (red line) where λ_{max} = 577 nm shows a perfect sample without any surface traps, and the stock shift is about 27 nm. This observed difference in stock shift from undoped to doped MAA-QDs is due to the existence of a d level of Co^{2+} ion, which changes the electronic transition producing a type of coupling with the sp level of CdSe nanocrystals; this coupling is called sp−d.

dx.doi.org/10.1021/tx2000015 |*Chem. Res. Toxicol.* 2011, 24, 640–650

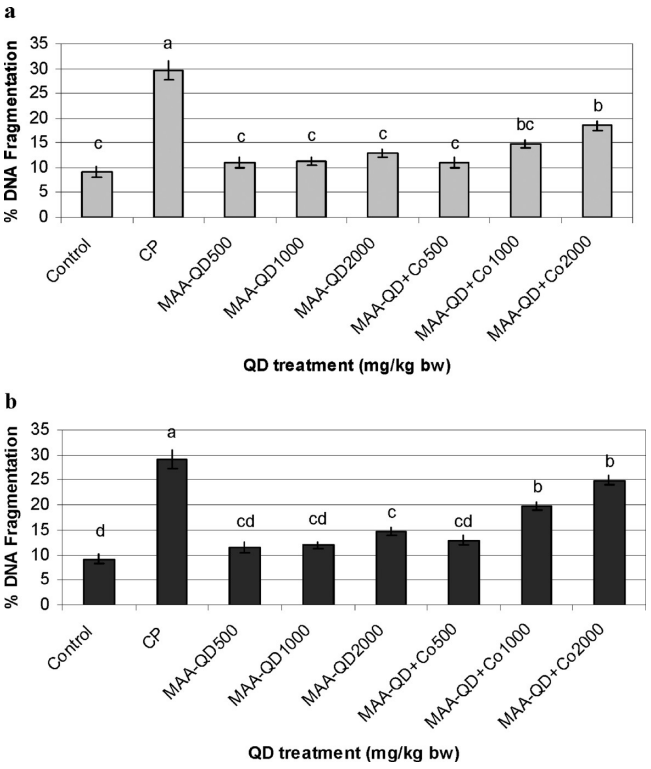

Figure 7. DNA fragmentation in liver tissues of male mice collected after 2 (a) and 7 days (b) of MAA-QD treatment analyzed by the diphenylamine reaction procedure. Results are expressed as the mean ± SEM of data from at least ten samples. a,b,c,d,cd: mean values within tissue with unlike lowercase letters were significantly different ($P < 0.05$, Scheffé-Test). c,b,cd: mean values within tissue with similar lowercase letters were not significant differences ($P > 0.05$). CP, cyclophosphamide; MAA, mercapto-acetic acid; QD, quantum dots; Co, cobalt.

Table 2. Micronucleated Polychromatic Erythrocytes (MnPCEs) of Male Mice Exposed to MAA-QDs for Different Time Intervals (Mean ± SEM)[a]

		MnPCEs/3000 PCEs	
treatment	concn (mg/kg)	2 days	7 days
control		7.4 ± 0.3 c	7.3 ± 0.5 c
cyclophosphamide[b]		25.3 ± 1.7 a	22.1 ± 1.3 a
undoped MAA-QDs[b]	500	7.8 ± 0.9 c	8.4 ± 0.9 c
	1000	8.6 ± 0.9 bc	9.8 ± 0.9 bc
	2000	9.7 ± 1.0 bc	14.7 ± 1.0 b
doped MAA-QDs[b]	500	7.8 ± 0.8 c	11.6 ± 1.1 bc
	1000	11.6 ± 0.9 bc	15.1 ± 1.0 b
	2000	13.9 ± 1.0 b	19.8 ± 1.2 a

[a] Mean values within columns with unlike lowercase letters (a,b,c) were significantly different ($P < 0.05$, Scheffé-Test). Mean values within columns with similar lowercase letters (c,b,bc) were not significant differences ($P > 0.05$). [b] Cyclophosphamide and MAA-QDs were injected as a single dose, and then the bone marrow cells were collected after 2 and 7 days of treatment.

Figure 5 shows the magnetic behavior of the three doses used in the *in vivo* study. It is clearly shown that the magnetic moment varies according to the dose weight where the amount of the magnetic materials changed from one dose to the other. The

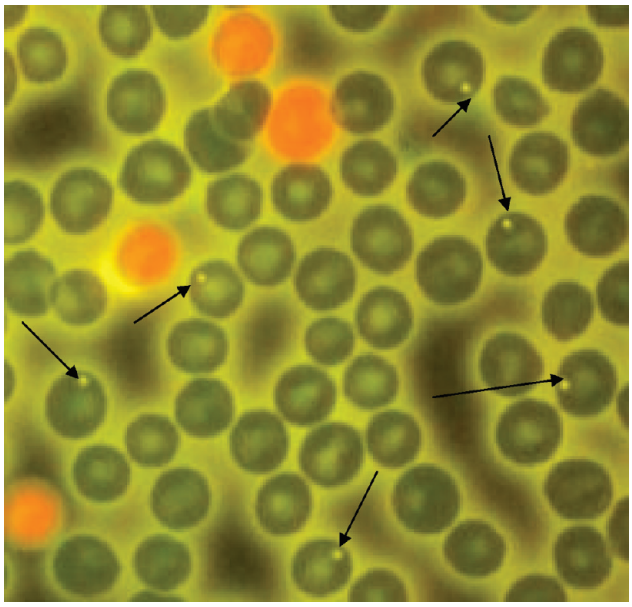

Figure 8. Acridine orange stained bone marrow erythrocytes of male mice. Arrow: micronucleated polychromatic erythrocyte (MnPCEs).

average switching field coercive field (H_C) was about 0.0053 T (53.5 Oe). The hysteresis loop shows a ferromagnetic behavior due to the doping of QDs with Co^{2+} ions.

To our knowledge, there are no data regarding the genotoxic effect of MAA-QDs on mammals *in vivo*. Dubertret et al. reported that QDs have little effect on cell viability, morphology, function, or development over the duration of the *in vivo* experiments at their concentrations optimized for labeling efficiency.[19] Gagné et al.[45] reported that genotoxic effects of cadmium-telluride (CdTe) quantum dots on freshwater mussels were observed.

The results obtained in this study (summarized in Figures 6−9 and Table 2) demonstrate the different toxicological properties of both pure and doped MAA-QDs. Genotoxic mechanism of action of the QDs needs more extensive studies to be fully understood. Cytotoxicity and genotoxicity of QDs has been observed in a large number of *in vitro* studies,[20,22,23,46−49] affecting cell growth and viability.[50] The extent of cytotoxicity has been found to be dependent upon a number of factors including size, capping materials, color, dose of QDs, surface chemistry, coating bioactivity, and processing parameters.[50−52]

Gao et al.[13] and Akerman et al.[53] reported that a substantial loss of QDs fluorescence over time was noted upon administration of QDs to living animals. Although the exact origin of the loss of QDs fluorescence was not clear, Gao et al.[13] stated that QD surface ligands and coatings were slowly degraded *in vivo*, leading to surface defects and fluorescence quenching. Similarly, Chen and Gerion[50] attributed the lack of observable genotoxicity of QDs to a surface coating, which successfully prevented the interaction of Cd, Se, Zn, and sulfur with proteins and DNA in the nucleus. In the present study, QDs were coated with mercapto-acetic acid molecules which may have the potential to prevent the direct interaction between QDs and biomolecules of male mice up to two days after treatment.

QD toxicity depends on multiple factors derived from both individual QD physicochemical properties and environmental conditions: oxidative, photolytic, and mechanical stability have each been shown to be determining factors in QD toxicity. Hardman[52]

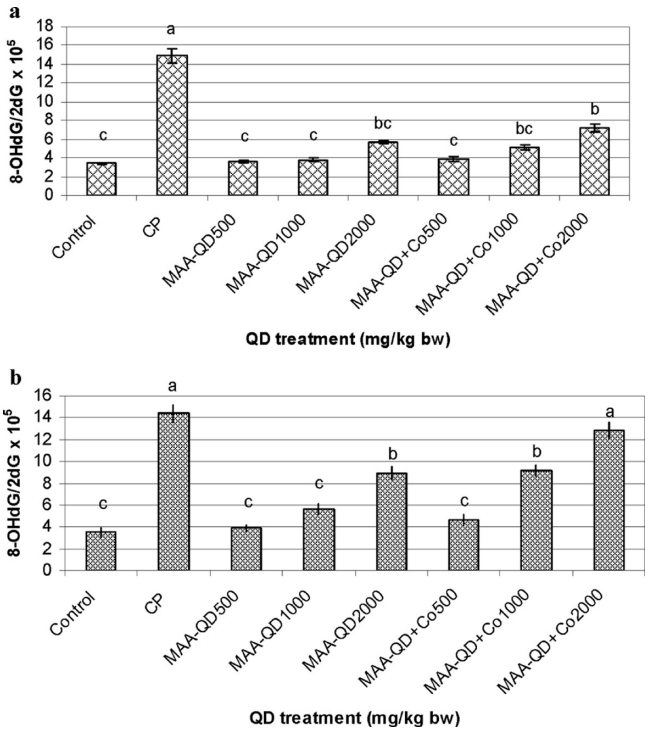

Figure 9. Generation of 8-OHdG in hepatic mice genome following MAA-QDs treatment. Liver tissue was harvested at the indicated time points (2 (a) and 7 days (b)), DNA extracted, and HPLC performed. DNA damage was expressed as the ratio of oxidized DNA base (8-OHdG) to nonoxidized base (2-dG) in liver DNA. Results are expressed as the mean ± SEM of data from at least ten samples. a,b,c: mean values within tissue with unlike lowercase letters were significantly different ($P < 0.05$, Scheffé-Test). b,c,bc: mean values within tissue with similar lowercase letters were not significantly different ($P > 0.05$). CP, cyclophosphamide; MAA, mercapto-acetic acid; QD, quantum dots; Co, cobalt.

reported that some QDs have been found to be cytotoxic only after oxidative and/or photolytic degradation of their core coatings.

In addition, He et al.[54] reported that nanoparticles tend to agglomerate when suspended in a low pH liquid producing an alteration of their surface ionic composition. This might cause the nanoparticles to separate from their agglomerates and produce an increased surface area, potentially increasing the generation of a cellular ROS. QDs may be degraded after several days in the living cells where the fluorescent intensity of cells was observed to gradually decrease.[52,55−57] QD degradation may occur due to low pH or oxidation of QD surface structures, or intracellular factors may be adsorbed onto QD surfaces. In the present study, the MAA-QDs were exposed to low pH because they were administered orally to male mice and then passed to the gastric tract. Therefore, MAA-QDs may be degraded, and their coating molecules are damaged between 2 to 7 days of treatment. Consequently, it may be presumed that induction of DNA damage and generation of high amounts of 8-OHdG were probably caused by the alteration of QD surface ionic composition and/or high intracellular ROS generation.

However, increasing DNA damage, MnPCEs formation, and generation of high amounts of 8-OHdG in male mice following the treatment of MAA-QDs coated with cobalt may be attributed to an indirect mechanism between free Co ions or Co ions on the QDs and DNA molecules.

Data addressing the genotoxic effects of Co inducing DNA damage have focused only on cobalt metal or compounds in soluble forms. However, studies investigating the genotoxic effects of Co-nanoparticles *in vivo* are still missing or sparse. De Boeck et al.[58] explored the *in vitro* genotoxicity of Co metal and compared it with that of hard metal particles in terms of concentration and time dependency. Co metal and cobalt chloride produced approximately the same level of DNA damage.

De Boeck et al.[58] assessed the ability of powder mixtures of Cr_3C_2, Mo_2C, and NbC with cobalt to induce chromosome/genome mutations (MnPCEs formation) in human lymphocytes. The exact mechanism by which cobalt compounds induce micronuclei is not clear; it might be the consequence of direct clastogenic activity, but aneuploidogenic activity should not be overlooked given the literature data on cobalt(II).[59]

The different behavior of the two cobalt forms (Co-nano and Co^{2+}) likely suggests that Co-nano is a potential genotoxic carcinogen.[60] Ponti et al.[60] reported that formation of chromosomal aberrations, in the form of micronuclei, induced by Co-nano, is a process which leads to a stable mutation that with higher probability could trigger morphological transformation. On the basis of these findings, the increased DNA damage in our own study is likely to be attributed to Co ions on the QD nanoparticles.

Regarding the genotoxic effects of nanoparticles, the data are sparse and have to be well evaluated considering the different types of *in vitro* models and *in vivo* studies. In fact, a study on Co-nano, by Colognato et al.,[61] using both the alkaline comet assay and the micronucleus test, showed that in human peripheral leukocytes, there is a dose-dependent increase in the primary DNA damage for Co-nano but not for Co^{2+}, whereas when analyzing the frequency of micronucleated binucleated cells, both compounds show positive results.

Ponti et al.[60] found that uptake of Co-nano by mouse fibroblasts *in vitro* was observed to be more than Co^{2+}. This high quantity of Co-nano uptake, in comparison with that of ions, is possibly due to the chemical nature of Co-nano since the particle surface may interact with proteins present in the culture medium and be more readily taken up by cells.[62] This type of internalization process due to nanoprotein interaction is also suggested by Limbach et al.,[63] who indicate that the particles could efficiently enter the cells by a Trojan horse-type mechanism.[63]

The genotoxic activity of Co seems to be due to the production of ROS.[64] Mao et al.[65] and Zou et al.[66] showed that the oxidative potential of Co^{2+} (10^{-3} M) and $CoCl_2$ could be modulated by chelator agents that interfere with the ability to produce ROS in H_2O_2-treated cells. The addition of antioxidants in culture media blunted these effects, suggesting that the apoptotic process is mediated by free radical generation. Besides free radical generation, several authors emphasized that magnetic nanoparticles preferentially localize at the mitochondrial level, altering oxidative phosphorylation.[67−69]

5. CONCLUSIONS

The present work has been devoted to study the genotoxic effect of CdSe-QDs and CdSe-QDs+Co. Our results indicated that the LD_{50} in both cases is more than 2000 mg/kg bw. Since much lower dose of CdSe QDs such as 500 mg/kg bw (i.e., 0.05 LD_{50}) could be used in biomedical imaging, this might mean that using such a dose of CdSe QDs for biomedical imaging is safe. Our findings support several *in vivo* imaging, clearance, and toxicity studies which used lower doses of QD-NPs such as

40pmol,[70] 2 μmol/kg,[71] and 45 nmol[72] than ours. This demonstrates that at significantly lower doses, these QD exposures may be useful for the biomedical field without the concern of toxicity because toxic levels in this work occurred at much higher doses.

Very high doses of MAA-QDs undoped and doped with cobalt (>500 mg/kg bw in case of doped MAA-QD+Co and 2000 mg/kg bw in the case of pure MAA-QD) were able to induce genotoxicity in mice tissues. It may be presumed that induction of DNA damage and generation of high amounts of 8-OHdG were probably caused by the alteration of QD surface ionic composition and/or high intracellular ROS generation. This means that pure CdSe QDs are much less toxic than cobalt-doped CdSe QDs.

AUTHOR INFORMATION

Corresponding Author

*Cell Biology Department, Genetic Engineering and Biotechnology Division, National Research Center (NRC), El.Tahrir Street, 12622 Dokki, Giza, Egypt. Phone: +2012-7410600. Fax: +202-33370931. E-mail: wagdykh@yahoo.com.

Funding Sources

This study was supported by Swedish research foundation SIDA under grant number 348-2007-6992.

DISCLOSURE

We have no other relevant affiliations or financial involvement with any organization or entity with a financial interest in or financial conflict with the subject matter or materials discussed in the manuscript apart from those disclosed. No writing assistance was utilized in the production of this manuscript.

ACKNOWLEDGMENT

We thank all the colleagues in Animal House, National Research Centre, Dokki, Giza, for taking care of the animals throughout the experiments.

REFERENCES

(1) Bruchez, J. M., Moronne, M., Gin, P., Weiss, S., and Alivisatos, A. P. (1998) Semiconductor nanocrystals as fluorescent biological labels. *Science 281*, 2013–2016.

(2) Bentolila, L. A. (2009) Quantum dots for in vivo small-animal imaging. *J. Nucl. Med. 50*, 4.

(3) Drbohlavova, J. (2009) Quantum dots: characterization, preparation and usage in biological systems. *Int. J. Mol. Sci. 10*, 656–673.

(4) Chao, W., Xue, G., and Xingguang, S. (2010) Study the damage of DNA molecules induced by three kinds of aqueous nanoparticles. *Talanta 80*, 1228–1233.

(5) Zhang, J. (2010) Fluorescent quantum dot-labeled aptamer bioprobes specifically targeting mouse liver cancer cells. *Talanta 81*, 505–509.

(6) Smith, A. M., and Nie, S. M. (2004) Chemical analysis and cellular imaging with quantum dots. *Analyst 129*, 672–677.

(7) Ma, Q., Su, X. G., Wang, X. Y., Wan, Y., Wang, C. L., and Yang, B (2005) et al. Fluorescence resonance energy transfer in doubly-quantum dot labeled IgG system. *Talanta 67*, 1029–1034.

(8) Michalet, X., Pinaud, F. F., Bentolila, L. A., Tsay, J. M., Doose, S., and Li, J. J. (2005) et al. Quantum dots for live cells, in vivo imaging, and diagnostics. *Science 307*, 538–544.

(9) Liang, J., Huang, S., Zeng, D., He, Z., Ji, X., and Ai, X. (2006) et al. CdSe quantum dots as luminescent probes for spironolactone determination. *Talanta 69*, 126–130.

(10) Chan, W. C. W., and Nie, S. (1998) Quantum dot bioconjugates for ultrasensitive nonisotopic detection. *Science 281*, 2016–2018.

(11) Weng, J., Song, X., Li, L., Qian, H., Chenb, K., and Xu, X. (2003) et al. Functional hybrid devices of proteins and inorganic nanoparticles. *Talanta 42*, 5796–5800.

(12) Wu, X. Y., Liu, H. J., Liu, J. Q., Haley, K. N., Treadway, J. A., and Larson, J. P. (2003) et al. The application on binders in low vulnerability ammunition. *Nat. Biotechnol. 21*, 41–42.

(13) Gao, X., Cui, Y., Levenson, R. M., Chung, L. W. K., and Nie, S. (2004) In vivo cancer targeting and imaging with semiconductor quantum dots. *Nat. Biotechnol. 22*, 969–976.

(14) Han, M., Gao, X., Su, J. Z., and Nie, S. (2001) Quantum-dot-tagged microbeads for multiplexed optical coding of biomolecules. *Nat. Biotechnol. 19*, 631–635.

(15) Jin, W. J., Fernandez-Arguelles, M. T., Costa-Fernandez, J. M., Pereiro, R., and Sanz-Medel, A. (2005) Photoactivated luminescent CdSe quantum dots as sensitive cyanide probes in aqueous solutions. *Chem. Commun.* 883–885.

(16) Lu, Q., Hu, S., Pang, D., and He, Z. (2005) Direct electrochemistry and electrocatalysis with hemoglobin in water-soluble quantum dots film on glassy carbon electrode. *Chem. Commun.* 2584–2585.

(17) Zhang, F., Li, C., Li, X., Wang, X., Wan, Q., and Xian, Y. (2006) et al. ZnS quantum dots derived a reagentless uric acid biosensor. *Talanta 68*, 1353–1358.

(18) Liang, J., He, Z., Zhang, S., Huanga, S., Ai, X., and Yang, H. (2007) et al. Study on DNA damage induced by CdSe quantum dots using nucleic acid molecular "light switches" as probe. *Talanta 71*, 1675–1678.

(19) Dubertret, B., Skourides, P., Norris, D. J., Noireaux, V., Brivanlou, A. H., and Libchaber, A. (2005) In vivo imaging of quantum dots encapsulated in phospholipid micelles. *Science 298*, 1759–1762.

(20) Derfus, A. M., Chan, W. C. W., and Bhatia, S. N. (2004) Probing the cytotoxicity of semiconductor quantum dots. *Nano Lett. 4*, 11–18.

(21) Hoshino, A., Fujioka, K., Oku, T., Suga, M., Sasaki, Y. F., and Ohta, T. (2004) et al. Physicochemical properties and cellular toxicity of nanocrystal quantum dots depend on their surface modification. *Nano Lett. 4*, 2163–2169.

(22) Kirchner, C., Liedl, T., Kudera, S., Pellegrino, T., Javier, A. M., and Gaub, H. E. (2005) et al. Cytotoxicity of colloidal. CdSe and CdSe/ZnS nanoparticles. *Nano Lett. 5*, 331–338.

(23) Lovrić, J., Bazzi, H. S., Cuie, Y., Fortin, G. R. A., Winnik, F. M., and Maysinger, D. (2005) Differences in subcellular distribution and toxicity of green and red emitting CdTe quantum dots. *J. Mol. Med. 83*, 377–385.

(24) Green, M., and Howman, E. (2005) Semiconductor quantum dots and free radical induced DNA nicking. *Chem. Commun. 7*, 121–123.

(25) Klimov, V. I. (2003) Nanocrystal Quantum Dots From fundamental photophysics to multicolor lasing. *Los Alamos Sci.* (28), 214–220.

(26) Gmez, D. E., Embden, J. V., Jasieniak, J., Smith, T. A., and Mulvaney, P. (2006) Blinking and surface chemistry of single CdSe nanocrystals. *Small 2*, 204–208.

(27) Efros, A. (2002) *Auger Processes in Nanosize Semiconductor Crystals*, Naval Research Laboratory, Washington, DC.

(28) Schmid, G. (2004) *Nanoparticles: From Theory to Application*, Vol. 8, Wiley-VCH Verlag GmbH & Co. KGaA, Weinheim, Germany.

(29) Empedocles, S. A., and Bawendi, M. G. (1999) Influence of spectral diffusion on the line shapes of single CdSe nanocrystallite quantum dots. *J. Phys. Chem. B 103*, 1826–1830.

(30) Nirmal, M., and Brus, L. (1999) Luminescence photophysics in semiconductor nanocrystals. *Acc. Chem. Res. 32*, 407–414.

(31) Mahler, B., Spincelli, P., Buil, S. P., Quelin, X., Hermier, J. P., and Dubertret, B. (2008) Towards non-blinking colloidal quantum dots. *Nat. Mater. 7*, 660–664.

(32) Spinicelli, P., Mahler, B., Buil, S. P., Qu, Lin X., Dubertret, B., and Hermier, J. P. (2009) Non-blinking semiconductor colloidal quantum dots for biology, optoelectronics and quantum optics. *Chem. Phys. Chem. 10*, 879–882.

(33) Yu, Z. H., Guo, L., Du, H., Krauss, T., and Silcox, J. (2005) Shell distribution on colloidal CdSe/ZnS quantum dots. *Nano Lett. 5*, 565–570.
(34) Murray, C. B., Norris, D. J., and Bawendi, M. G. (1993) Synthesis and characterization of nearly monodisperse CdE (E = S, Se, Te) semiconductor nanocrystallites. *J. Am. Chem. Soc. 115*, 8706–8715.
(35) Peng, Z. A., and Peng, X. (2001) Formation of high-quality CdTe, CdSe, and CdS nanocrystals using CdO as precursor. *J. Am. Chem. Soc. 123*, 183.
(36) Qu, L., Peng, Z. A., and Peng, X. (2001) Alternative routes toward high quality CdSe nanocrystals. *Nano Lett. 1*, 333–337.
(37) Mohamed, M. B., Tonti, D., Al-Salman, A., Chemseddine, A., and El-Chagui, M. (2005) Synthesis of high quality zinc-blende CdSe nanocrystals. *J. Phys. Chem. 10*, 10533–10537.
(38) The Organisation for Economic Co-operation and Development (2001) *Guidelines 420: Acute Oral Toxicity: Fixed Dosed Procedure, December, 2001*.
(39) Burton, K. (1956) A study of the conditions and mechanism of the diphenylamine reaction for the colorimetric estimation of deoxyribonucleic acid. *Biochem. J. 62*, 315–323.
(40) Lu, T., Xu, Y., Mericle, M. T., and Mellgren, R. L. (2002) Participation of the conventional calpains in apoptosis. *Biochim. Biophys. Acta 1590*, 16–26.
(41) Ueda, T., Hayashi, M., Koide, N., Sofuni, T., and Kobayashi, J. (1992) A preliminary study of the micronucleus test by acridine orange fluorescent staining compared with chromosomal aberration test using fish erythropoietic and embryonic cells. *Water Sci. Technol. 25*, 235–240.
(42) Patel, M., Liang, L. P., and Roberts, L. J. (2001) Enhanced hippocampal F2-isoprostane formation following kainateinduced seizures. *J. Neurochem. 79*, 1065–1069.
(43) SAS (1982) *SAS User'S Guide: Statistics Edition*, SAS Institute Inc., Cary, NC.
(44) Brus, L. E. (1986) Electronic wave-functions in semiconductor clusters: experiment and theory. *J. Phys. Chem. 90*, 2555–2560.
(45) Gagné, F., Auclair, J., Turcotte, P., Fournier, M., Gagnon, C., Sauvé, S., and Blaise, C. (2008) Ecotoxicity of CdTe quantum dots to freshwater mussels: Impacts on immune system, oxidative stress and genotoxicity. *Aquatic Toxicol. 86*, 333–340.
(46) Medintz, I. L., Uyeda, H. T., Goldman, E. R., and Mattoussi, H. (2005) Quantum dot bioconjugates for imaging, labelling and sensing. *Nat. Mater. 4*, 435–446.
(47) Clarke, S. J., Hollmann, C. A., Zhang, Z., Suffern, D., Bradforth, S. E., and Dimitrijevic, N. M. (2006) et al. Photophysics of dopamine-modified quantum dots and effects on biological systems. *Nat. Mater. 5*, 409–417.
(48) Hsieh, S. C., Wang, F. F., Hung, S. C., Chen, Y., and Wang, Y. J. (2006) The internalized CdSe/ZnS quantum dots impair the chondrogenesis of bone marrow mesenchymal stem cells. *J. Biomed. Mater. Res., Part B 79*, 95–101.
(49) Singh, N., Manshian, B., Jenkins, G. J., Griffiths, S. M., Williams, P. M., Maffeis, T. G., Wright, C. J., and Doak, S. H. (2009) NanoGenotoxicology: the DNA damaging potential of engineered nanomaterials. *Biomaterials 30*, 3891–914.
(50) Chen, F. Q., and Gerion, D. (2004) Fluorescent CdSe/ZnS nanocrystal-peptide conjugates for long-term, nontoxic imaging and nuclear targeting in living cells. *Nano Lett. 4*, 1827–1832.
(51) Shiohara, A., Hoshino, A., Hanaki, K., Suzuki, K., and Yamamoto, K. (2004) On the cyto-toxicity caused by quantum dots. *Microbiol. Immunol. 48*, 669–675.
(52) Hardman, R. (2006) A toxicologic review of quantum dots: toxicity depends on physicochemical and environmental factors. *Environ. Health Perspect. 114*, 165–172.
(53) Akerman, M. E., Chan, W. C. W., Laakkonen, P., Bhatia, S. N., and Ruoslahti, E. (2002) Nanocrystal targeting in vivo. *Proc. Natl. Acad. Sci. U.S.A. 99*, 12617–12621.
(54) He, Y. T., Wan, J., and Tokunga, T. (2008) Kinetic stability of hematite nanoparticles: the effect of particle. *J. Nanopart. Res. 10*, 321–332.
(55) Powers, K. W., Brown, S. C., Krishna, V. B., Wasdo, S. C., Moudgil, B. M., and Roberts, S. M. (2006) Research strategies for safety evaluation of nanomaterials. Part VI. Characterization of nanoscale particles for toxicological evaluation. *Toxicol. Sci. 90*, 296–303.
(56) Fischer, H. C., and Chan, W. C. W. (2007) Nanotoxicity: the growing need for in vivo study. *Curr. Opin. Biotechnol. 18*, 565–571.
(57) Aillon, K. L., Xie, Y., El-Gendy, N., Berkland, C. J., and Laird Forrest, M. (2009) Effects of nanomaterial physicochemical properties on in vivo toxicity. *Adv. Drug Delivery Rev. 61*, 457–466.
(58) De Boeck, M., Lombaert, N., De Backer, S., Finsy, R., Lison, D. M., and Kirsch-Volders, M. (2003) In vitro genotoxic effects of different combinations of cobalt and metallic carbide particles. *Mutagenesis 18*, 177–186.
(59) De Boeck, M., Kirsch-Volders, M., and Lison, D. (2003) Cobalt and antimony: genotoxicity and carcinogenicity. *Mutat. Res. 533*, 135–152.
(60) Ponti, J., Sabbioni, E., Munaro, B., Broggi, F., Marmorato, P., Franchini, F., Colognato, R., and Rossi, F. (2009) Genotoxicity and morphological transformation induced by cobalt nanoparticles and cobalt chloride: an in vitro study in Balb/3T3 mouse fibroblasts. *Mutagenesis 24*, 439–445.
(61) Colognato, R., Bonelli, A., Ponti, J., Farina, M., Bergamaschi, E., Sabbioni, E., and Migliore, L. (2008) Comparative genotoxicity of cobalt nanoparticles and ions on human peripheral leukocytes in vitro. *Mutagenesis 23*, 1–6.
(62) Oberdörster, G., Maynard, A., and Donaldson, K. (2005) et al. A report from the ILSI Research Foundation/Risk Science Institute National Toxicity Screening Working Group. Principles for characterizing the potential human health effects from exposure to nanomaterials: elements of a screening strategy. *Part. Fibre Toxicol. 6*, 2–8.
(63) Limbach, L. K., Wick, P., Manser, P., Grass, R. N., Bruinink, A., and Stark, W. J.n (2007) Exposure of engineered nanoparticles to human lung epithelial cells: influence of chemical composition and catalytic activity on oxidative stress. *Environ. Sci. Technol. 41*, 3791–3792.
(64) Lison, D., De Boeck, M., Verougstraete, V., and Kirsch-Volders, M. (2001) Update on the genotoxicity and carcinogenicity of cobalt compounds. *Occup. Environ. Med. 58*, 619–625.
(65) Mao, Y., Liu, K. J., Jiang, J. J., and Shi, X. (1996) Generation of reactive oxygen species by Co(II) from H_2O_2 in the presence of chelators in relation to DNA damage and 2′-deoxyguanosine hydroxylation. *J. Toxicol. Environ. Health 47*, 61–75.
(66) Zou, W., Yan, M., Xu, W., Huo, H., Sun, L., Zheng, Z., and Liu, Z. (2001) Cobalt chloride induces PC12 cells apoptosis through reactive oxygen species and accompanied by AP-1 activation. *J. Neurosci. Res. 64*, 646–653.
(67) Foley, S., Crowley, C., Smaihi, M., Bonfils, C., Erlanger, B. F., Seta, P., and Larroque, C. (2002) Cellular localisation of a water-soluble fullerene derivative. *Biochem. Biophys. Res. Commun. 294*, 116–119.
(68) Li, N., Sioutas, C., and Cho, A (2003) et al. Ultrafine particulate pollutants induce oxidative stress and mitochondrial damage. *Environ. Health Perspect. 111*, 455–460.
(69) Savic, R., Luo, L., Eisenberg, A., and Maysinger, D. (2003) Micellar nanocontainers distribute to defined cytoplasmic organelles. *Science 300*, 615–618.
(70) Yang, R. S., Chang, L. W., Wu, J. P., Tsai, M. H., Wang, H. J., Kuo, Y. C., Yeh, T. K., Yang, C. S., and Lin, P. (2007) Persistent tissue kinetics and redistribution of nanoparticles, quantum dot 705, in mice: ICP-MS quantitative assessment. *Environ. Health Perspect. 115*, 1339–1343.
(71) Zhang, Y., Chen, W., Zhang, J., Liu, J., Chen, G., and Pope, C. (2007) *In vitro* and *in vivo* toxicity of CdTe nanoparticles. *J. Nanosci. Nanotechnol. 7*, 497–503.
(72) Hauck, T. S., Anderson, R. E., Fischer, H. C., Newbigging, S., and Chan, W. C. (2010) *In vivo* quantum-dot toxicity assessment. *Small 6*, 138–144.